JOURNAL OF BACTERIOLOGY, July 2006, p. 5204–5211 Vol. 188, No. 14
0021-9193/06/$08.00+0 doi:10.1128/JB.00387-06
Copyright © 2006, American Society for Microbiology. All Rights Reserved.

Constitutive Activation of Two-Component Response Regulators: Characterization of VirG Activation in *Agrobacterium tumefaciens*

Rong Gao, Aindrila Mukhopadhyay,§ Fang Fang, and David G. Lynn*

Center for Fundamental and Applied Molecular Evolution, Departments of Chemistry and Biology, Emory University, Atlanta, Georgia 30322

Received 17 March 2006/Accepted 27 April 2006

Response regulators are the ultimate modulators in two-component signal transduction pathways. The N-terminal receiver domains generally accept phosphates from cognate histidine kinases to control output. VirG for example, the response regulator of the VirA/VirG two-component system in *Agrobacterium tumefaciens*, mediates the expression of virulence genes in response to plant host signals. Response regulators have a highly conserved structure and share a similar conformational activation upon phosphorylation, yet the sequence and structural features that determine or perturb the cooperative activation events are ill defined. Here we use VirG and the unique features of the *Agrobacterium* system to extend our understanding of the response regulator activation. Two previously isolated constitutive VirG mutants, VirGN54D and VirGI77V/D52E, provide the foundation for our studies. In vivo phosphorylation patterns establish that VirGN54D is able to accumulate phosphates from small-molecule phosphate donors, such as acetyl phosphate, while the VirGI77V/D52E allele carries conformational changes mimicking the active conformation. Further structural alterations on these two alleles begin to reveal the changes necessary for response regulator activation.

Two-component regulatory systems, composed of a histidine sensor kinase and a response regulator (RR), mediate adaptive responses in a wide variety of cellular processes, such as chemotaxis, sporulation, quorum sensing, and pathogenesis (43, 50). The response regulator usually lies at the end of the two-component pathway, functioning as a phosphorylation-dependent modulator. Generally, the N-terminal receiver domain receives phosphate from the cognate histidine autokinase upon signal input, and the C-terminal effector domain regulates output. This modular organization of histidine kinase/RR has been repeatedly exploited and greatly diversified to the point that it underlies most prokaryotic environmental sensing.

Despite the great diversity of histidine kinase input domains and the C-terminal effector output domains, the receiver domains of RRs share a remarkably conserved structure fold and appear to follow a similar conformational change/activation following phosphorylation (1–3, 9, 15, 20, 21, 43). These receiver domains contain a doubly wound α/β fold with a central five-stranded β sheet surrounded by five α helices. The conserved Asp at the β3-α3 loop, together with two other carboxylate-containing side chains (Asp or Glu) at the β1-α1 loop, a Ser or Thr at the β4-α4 loop, and a Lys at the β5-α5 loop, make up the highly conserved phosphorylation center. Phosphorylation causes little change in overall secondary structure but rather induces a repositioning of secondary structural elements in the β4-α4-β5-α5 region—a substantial restructuring of the molecular surface. The mechanism for such repositioning or conformational propagation appears conserved as well, involving an Asp-Ser/Thr-Tyr/Phe "aromatic switch" (3, 15, 22) that results in the rearrangement of the β4-α4-β5-α5 region by altering the orientation and packing around a conserved aromatic residue (Tyr or Phe).

It has been suggested that RRs exist in an equilibrium composed of the "inactive" and "active" conformations, and this equilibrium is shifted towards the active conformation upon phosphorylation (9, 47). Apparently, individual response regulators in various systems have evolved to maintain their different lifetimes of active forms to match individual biological roles, even though they have a similar structure fold and conformational propagation pathway. For example, the half-life of the phosphorylated RR ranges from 0.5 min in CheY (*Escherichia coli*) to 180 min in Spo0F (*Bacillus subtilis*), corresponding to the timescales of chemotactic behaviors (seconds) and sporulation (hours), respectively (25, 55). Different lifetimes of phosphorylated RRs may well represent different equilibrium constants evolved to adopt individual RRs for specific cellular processes. At the limits, mutations could shift such conformation equilibrium to either a complete loss of activity or a constitutive activation. In this context, constitutively active alleles are particularly interesting, as they should reveal evolutionarily critical residues for maintaining the conformation equilibrium in the "on" extreme. We reasoned that analyzing and comparing these constitutive mutants may reveal additional critical structural features necessary for activation and may distinguish essential features associated with the dynamics of individual response regulators.

The VirA/VirG two-component system in *Agrobacterium tumefaciens* represents a rich system to explore such constitutive alleles. VirG has been the subject of extensive mutagenesis, and in vivo phosphorylation protocols have been established (10–12, 30, 33, 35, 36). All the input signals, acidic pH, monosaccharides, and phenols (e.g., acetosyringone [AS]), responsible for sensing plant hosts and mediating the transfer of oncogenic DNA into the plant genome are known (44, 52, 56).

* Corresponding author. Mailing address: Center for Fundamental and Applied Molecular Evolution, Departments of Chemistry and Biology, Emory University, 1515 Dickey Drive, Atlanta, GA 30322. Phone: (404) 727-9348. Fax: (404) 727-6586. E-mail: dlynn2@emory.edu.

§ Present address: Physical Biosciences Division, Lawrence Berkeley National Laboratory, Berkeley CA 94720.

Downloaded from http://jb.asm.org/ on July 19, 2018 by guest

Phosphorylation of VirG is thought to induce dimerization and *vir* box binding to activate the expression of the virulence (*vir*) genes. Finally, VirG shares sequence similarities with the OmpR-PhoB subfamily of response regulators, and Asp52 has been shown to be the site of phosphorylation (14). Based on sequence homology, the conserved phosphorylation center residues of VirG include D8, D9, D52, S79, and K102. Indeed, alleles carrying substitutions at these residues, such as D8N, D52E, and S79G, and at other proximal residues, such as V51A, L53P, I100T, and F104S, result in the loss of VirG activity (35, 36).

Constitutively active mutants of VirG have been isolated with mutations at three positions, N54 (VirGN54D), I77 (VirGI77V and VirGI77V/D52E), and I106 (VirGI106L, VirGI106F, VirGI106P, and VirGI106Y) (10, 11, 13, 33, 36). Among these mutants, only VirGI77V/D52E and VirGN54D are no longer AS responsive, and therefore they are the focus of this investigation. The constitutive activity of VirGI77V/D52E appears unusual since the conserved phosphorylated D52 residue is altered. VirGN54D was shown not to be phosphorylated by the kinase VirA in vitro (13), and a maltose-binding protein (MBP)-VirGN54D chimera showed higher DNA binding affinity than MBP-VirG (wild type) (12), leading to the hypothesis that VirGN54D does not require phosphorylation for activity. It was suggested that the additional negative charge of N54D in the active site may mimic the phosphoryl group in activated VirG (12). However, the conserved D52 residue was still essential for the constitutive activity of VirGN54D, as alleles carrying the D52E mutation resulted in complete loss of activity (10, 33). As these alleles appear to have different dependencies on the conserved D52 residue, and possibly distinctive mechanisms, we initiated a more thorough examination of their activities.

TABLE 1. Bacterial strains and plasmids

Strain or plasmid	Relevant characteristics	Reference or source
Strains		
E. coli		
AJW678	*thi-1 thr-1*(Am) *leuB6 metF159*(Am) *rpsL136* Δ*lacX74*	17
AJW1939	AJW678 Δ*ackA*	17
A. tumefaciens		
A136	Strain C58 cured of pTi plasmid	49
Plasmids		
pJZ*A*	P_{virB}-*lacZ* into pMON596, IncP Sp^r	8
pRG129	*virA* in pJZ*A*, Sp^r	This study
pSW209Ω	*virB*::*lacZ*, IncP Sp^r	48
pYW15	Broad-host-range expression vector, IncW, pBR322*ori*, Ap^r	48
pYW47	P_{N25}-6xHis-*virG* in pYW15, Ap^r	48
pYW48	*virA* in pYW47, Ap^r	48
pAM13	P_{N25}-6xHis-*virG*(*N54D*) in pYW15, Ap^r	30
pRG80	P_{N25}-6xHis-*virG*(*N54D*) in pYW15 derivative, Ap^r	This study
pRG112b	P_{N25}-6xHis-*virG*(*I77V*/*D52E*) in pYW15, Ap^r	This study
pAM18	P_{N25}-6xHis-*virG*(*N54D*/*D52E*) in pYW15, Ap^r	This study
pAM19	P_{N25}-6xHis-*virG*(*D52E*) in pYW15, Ap^r	30
pAM20	*virA* in pAM18, Ap^r	This study
pAM21	*virA* in pAM19, Ap^r	30
pA1	P_{N25}-6xHis-*virG*(*N54D*/*D9A*) in pYW15, Ap^r	This study
pB1	P_{N25}-*virG*(*I77V*/*D52E*/*D9A*) in pYW15, Ap^r	This study
pC1	P_{N25}-6xHis-*virG*(*D9A*) in pYW15, Ap^r	This study
pRG111	P_{N25}-6xHis-*virG*(*I77V*) in pYW15, Ap^r	This study
pB7	P_{N25}-6xHis-*virG*(*I77V*/*D52L*) in pYW15, Ap^r	This study
pB8	P_{N25}-6xHis-*virG*(*I77L*/*D52E*) in pYW15, Ap^r	This study
pB9	P_{N25}-6xHis-*virG*(*I77A*/*D52E*) in pYW15, Ap^r	This study
pPS1.3	P_{lac}-*rpoA* from A136 into pTZ19R, ColE1, Ap^r	24
pET1	P_{lac}-*rpoA* into pET24 (Novagen), Km^r	This study
pRG145	P_{virB}-*lacZ* into pPS1.3, Ap^r	This study
pRG146	P_{virB}-*lacZ* into pET1, Km^r	This study
pRG149	P_{N25}-6xHis-*virG*(*I77V*/*D52E*), IncW Ap^r	This study
pFQ95	P_{N25}-6xHis-*virG*(*N54D*), Km^r	This study

MATERIALS AND METHODS

Bacterial strains and growth conditions. The bacterial strains used in this study are listed in Table 1. *E. coli* strains XL1-Blue (Stratagene) and DH5α (Invitrogen) were used for routine cloning and the construction of VirG mutants. *A. tumefaciens* strains were grown at 28°C in Luria-Bertani (LB) medium or induction medium (IM) (pH 5.5) (4) containing glucose. Additional supplements, such as antibiotics, AS, and isopropyl-β-D-thiogalactopyranoside (IPTG), were added when appropriate as indicated below.

Plasmid constructions. The plasmids used in this study are listed in Table 1. The reporter plasmid pRG129 was constructed by releasing *virA* as a KpnI piece from pVRA8 (19) and inserting into pJZ4. A constitutive promoter (P_{N25}) was used to drive the expression of all the *virG* alleles (48). pRG80 was created by inserting the NcoI piece from pAM13, containing P_{N25}-6xHis-*virGN54D*, into a pYW15 derivative. *virGN54D*/*D52* was amplified from pGP411 (10) using primers S-GON, 5′-GGGAGCTCAAACACGTTCTTCTTATC-3′ (SacI site underlined), and A-GON, 5′-GGGGTACCTCAGGCTGCCATCGTCCC-3′ (KpnI site underlined), followed by a complete KpnI digestion and a partial SacI digestion, since D52E introduced an additional SacI site in the *virG* open reading frame. Then the desired fragment was ligated into the SacI and KpnI-digested pYW15 to give pAM18. *virGI77V* and *virGI77V*/*D52E* were placed behind the P_{N25} promoter using a similar method with the above primers and pSG14/pSG13 (10) as templates, except for a minor modification for *virGI77V*/*D52E* in that the vector pYW15 was cut by SacI and treated with a Klenow fragment followed by digestion with KpnI and ligation with the KpnI-treated PCR product. The resultant pRG111 and pRG112b contain P_{N25}-6xHis-*virGI77V* and P_{N25}-6xHis-*virGI77V*/*D52E*, respectively. All the constructs involving PCR amplification were confirmed by sequencing.

Site-specific mutagenesis was performed using the recombinant PCR with specific primers for individual mutations. The primary PCRs were done using pYW47, pRG80, and pRG112b as templates with the following primers: (I) ECORIS, 5′-GCAGAATTCATTAAAGAGGAGAA-3′ (EcoRI site underlined) and the antisense primers containing the specific mutation; and (II) the sense mutation primers and AGK, 5′-GCGGTACCTCAGGCTGCCATCGTCCC-3′ (KpnI site underlined). Primary PCR products I and II were gel purified and mixed as templates for the secondary PCR with ECORIS and AGK as primers. The secondary PCR products containing the desired *virG* mutants were ligated into pYW15 as EcoRI and KpnI pieces to give the plasmids listed in Table 1. The specific mutations were confirmed by sequencing.

In order to observe *vir* expression in *E. coli* (23), a BamHI fragment containing P_{virB}-*lacZ* was ligated into pPS1.3, which has a P_{lac}-driven *rpoA* gene from *A. tumefaciens*, to give pRG145. Consequently, P_{N25}-6xHis-*virGI77V*/*D52E* and P_{N25}-6xHis-*virGN54D* were inserted into compatible plasmids that can coexist with pRG145.

β-Galactosidase assays for *vir* gene induction. For analyzing *vir* expression in *A. tumefaciens*, induction assays were conducted as described previously (8). *Agrobacterium* strains carrying reporter plasmid pRG129 or pSW209Ω together with plasmids containing the indicated *virG* alleles were cultured in IM (4) supplemented with 13 mM glucose at 28°C for 14 h. β-Galactosidase activity was then assayed as described previously (28). For assaying *vir* expression in *E. coli*, LB medium is used directly instead of IM due to the impaired growth of *E. coli* in IM. *E. coli* strains containing the indicated plasmids were grown in LB medium at 28°C for 14 h, and approximately 1 optical density unit at 600 nm of bacteria was pelleted, resuspended in 1 ml phosphate-buffered saline, and assayed subsequently (28).

In vivo protein phosphorylation. In vivo ^{32}P labeling of VirG proteins was performed as described previously (30). *Agrobacterium* strains were cultured in phosphate-deficient IM for overnight phosphate starvation (12 h). Then, $H_3{}^{32}PO_4$ (NEN Dupont) was added at a specific activity of 35 μCi/ml, and labeling was allowed to proceed for 3 h before the bacteria were harvested and lysed by sonication. The His_6-tagged VirG proteins were purified from the clarified lysates using Ni-nitrilotriacetic resins as per the QIAGEN protocol using 500 mM imidazole for elution. The eluants were resolved by 14% Tris-glycine sodium dodecyl sulfate-polyacrylamide gel electrophoresis gels (Invitro-

Downloaded from http://jb.asm.org/ on July 19, 2018 by guest

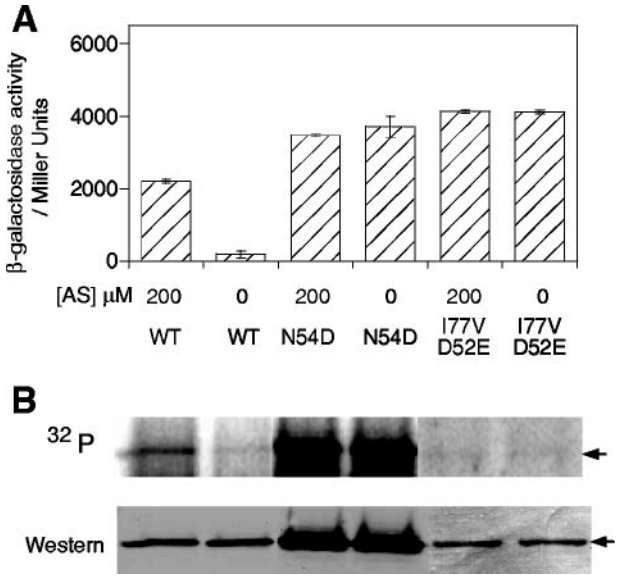

FIG. 1. P_{virB}-*lacZ* expression (A) and in vivo phosphorylation (B) of VirG mutants. *A. tumefaciens* A136 strains carrying pYW48 (wild type [WT]), pAM13 (N54D), or pRG112b (I77V/D52E) together with a P_{virB}-*lacZ* reporter plasmid were assayed in parallel with in vivo phosphorylation. Aliquots (1 ml) of phosphate-starved cultures were taken out, supplemented with phosphates, and incubated for 10 h prior to the β-galactosidase assay. The rest of the phosphate-starved cultures were used for in vivo phosphorylation. The phosphorimaging and Western blotting detected by anti-His are shown in the upper and lower lanes of panel B, respectively. Arrows mark the positions of VirG proteins.

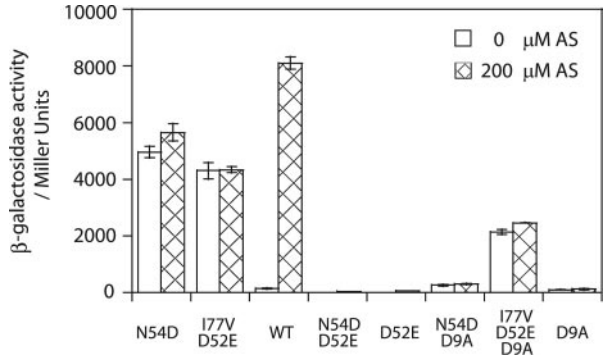

FIG. 2. P_{virB}-*lacZ* expression by VirG alleles with an additional D52E or D9A mutation. β-Galactosidase activity was assayed for A136(pRG129) strains containing a plasmid-borne *virA* and the following plasmids: (from left to right) pRG80, pRG112b, pYW47, pAM18, pAM19, pA1, pB1, and pC1. WT, wild type.

gen) and electro-blotted onto polyvinylidene difluoride (NEN Dupont) membranes for visualization by phosphorimaging (Amersham) and Western blot analyses using anti-penta-His monoclonal antibody (QIAGEN) (30).

Protein purification. To purify VirG proteins, plasmids carrying P_{N25}- driven His_6-tagged *virG* alleles were transformed into *E. coli* strain M15(pREP4) (QIAGEN). Overnight cultures (10 ml) were used to inoculate 600 ml of LB medium containing appropriate antibiotics and grown at 20°C until the optical density at 600 nm reached 0.6. IPTG was then added to a concentration of 300 μM, and the cultures were further incubated at 16°C for 12 h. Cells were centrifuged and resuspended in 10 ml of lysis buffer (50 mM Tris-HCl, 300 mM NaCl, 15 mM imidazole, pH 7.5) followed by sonication on ice for 3 min. The clarified lysates were passed through the Ni column packed with 3 ml of Ni-nitrilotriacetic resins (QIAGEN), and the columns were washed by the lysis buffer and washing buffer (lysis buffer plus 25 mM imidazole) until no significant amount of proteins was detected by Bradford assay (Pierce) in the fractions washed through. His-tagged VirG proteins were eluted with lysis buffer supplemented with 250 mM imidazole, and the concentrations were determined by Bradford assay. These protein samples were immediately used for gel retardation assays or precipitated using 30% ammonium sulfate and stored at −20°C for future use.

Gel retardation assays. The DNA fragment (~160 bp) containing the *virB* promoter was amplified from pRG129 using primers VIRB2, 5′-CGGAATTCT CTAGAACGGTACCTCTCCTTAGCTCGCAAC-3′ (XbaI site underlined), and VIRB4, 5′-GGTTCTCGGTCCATGTTTTGTTC-3′, and digested with XbaI. The fragment was then labeled with [α-^{32}P]dCTP in a Klenow reaction and purified by a QIAGEN nucleotide removal kit. Equal amounts of DNA were incubated with VirG proteins for 30 min at the indicated concentrations in the reaction buffer (50 mM HEPES, 10 mM $MgCl_2$, 50 mM KCl, 1 mM dithiothreitol, pH 7.4). The samples were resolved by 6% DNA retardation gel (Invitrogen) and analyzed by phosphorimaging.

Structure modeling. The structures of unphosphorylated RRs (protein database [PDB] entries: 1MVO, 1B00_A, 1QKK, 1DCK_B, and 1JBE) (2, 27, 38, 41) and phosphorylated or BeF_3^--treated RRs (PDB entries: 1L5Y_A, 1D5W_A, 1FQW_A, and 1QMP_A) (3, 20, 22, 32) were chosen as templates to model the unphosphorylated and phosphorylated VirG structures, respectively. Multiple sequences of response regulators were aligned with the CLUSTALW program, and the sequence alignments of VirG with these RRs were sent to SWISS-PROT (http://us.expasy.org/sprot) to generate the PDB files for VirG model structures.

RESULTS

In vivo phosphorylation of constitutive VirG alleles. *virG*, *virGN54D*, and *virGI77V/D52E* were placed behind a constitutive P_{N25} promoter to avoid autocatalytic expression by the native promoter (30, 48, 51). As shown in Fig. 1, the level of wild-type VirG remained constant (Fig. 1B, Western lane) and required AS to drive significant *vir* gene expression. When these cells were incubated with $H_3{}^{32}PO_4$ (Fig. 1B, ^{32}P lane), the phosphate on VirG accumulated significantly with AS induction, consistent with previous reports (30). However, both VirGN54D and VirGI77V/D52E were constitutively active in *vir* expression, independent of AS (Fig. 1A). Whereas VirGI77V/D52E did not show any detectable phosphorylation, VirGN54D was significantly phosphorylated independent of AS. Again consistent with previous reports, the N54D protein accumulates to consistently higher levels in these cells and its activity is independent of the histidine kinase VirA (30).

Alleles carrying the glutamate substitution (D52E) at the phosphorylation site, VirGD52E and VirGN54D/D52E, were inactive with or without AS (Fig. 2) and showed no in vivo phosphorylation (Fig. 3A). Asp9 (D9) is assigned as another of the five conserved residues within the phosphorylation active site, and substitutions at this position in other response regulators generally abolish or greatly reduce phosphorylation (25, 39). The same was observed for VirGD9A; *vir* gene expression was not induced by AS (Fig. 2), and the protein was not phosphorylated in vivo (Fig. 3B, lane 1). Introduction of D9A into VirGI77V/D52E resulted in little change in its constitutive activity (Fig. 2), suggesting that the D9A substitution did not disrupt the overall structural fold, and most importantly, that phosphorylation was not required for the constitutive activity of VirGI77V/D52E. VirGN54D/D9A however showed only residual activity (Fig. 2) and little phosphorylation (Fig. 3B, lane 2). Therefore, phosphorylation on the conserved D52 residue (Fig. 3C) appears essential for the constitutive activity of VirGN54D.

Downloaded from http://jb.asm.org/ on July 19, 2018 by guest

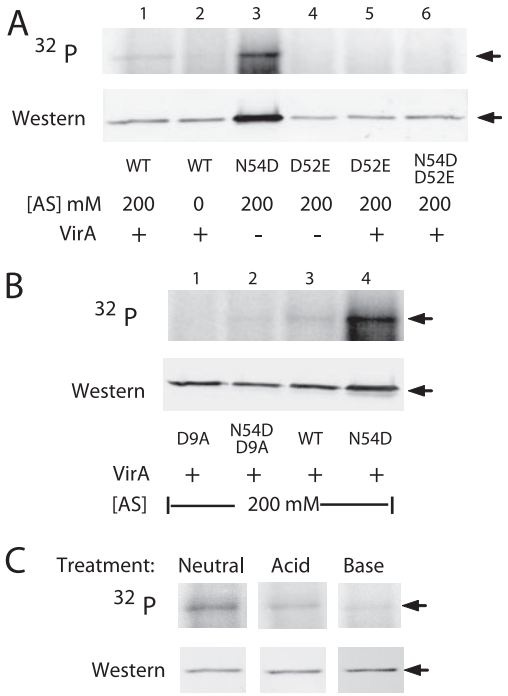

FIG. 3. Role of the conserved phosphorylation center in VirG phosphorylation. In vivo phosphorylation patterns of VirG alleles are shown in the upper panels, while protein expression profiles are shown in the lower panels. (A) Phosphorylation of VirGs with the D52E mutation. A136(pSW209Ω) strains carrying the following plasmids were used: lanes 1 and 2, pYW48; lane 3, pAM13; lane 4, pAM19; lane 5, pAM21; lane 6, pAM20 (lanes 1 and 2 were from Fig. 1 for comparative purposes). (B) Phosphorylation of VirGs with the D9A mutation. A136(pRG129) strains containing a plasmid-borne *virA* and the indicated plasmids were labeled with $H_3{}^{32}PO_4$ in the presence of 200 μM AS. Lane 1, pC1; lane 2, pA1; lane 3, pYW48; lane 4, pAM13. (C) Chemical stability of the phosphate on VirGN54D. Three identical membranes from ^{32}P-labeled A136(pRG129, pRG80) samples were incubated with Tris-buffered saline at pH 7.0 (Neutral), 1 M HCl (Acid), or 3 M NaOH (Base) for 2 h at room temperature prior to the phosphorimaging and Western blotting. WT, wild type.

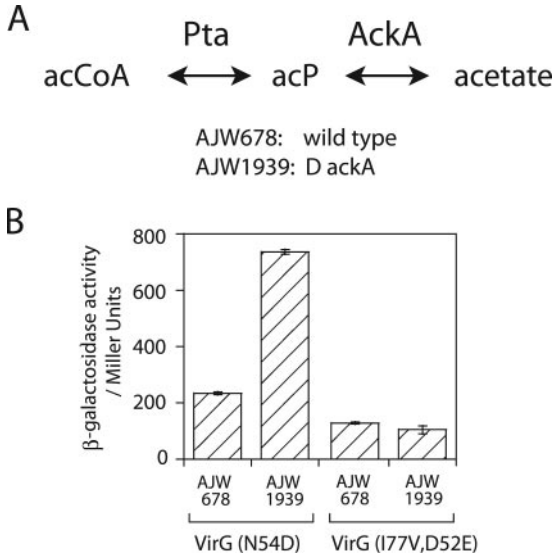

FIG. 4. P_{virB}-*lacZ* expression by VirG alleles in *E. coli* strains with mutations in the acetyl phosphate synthesis pathway. (A) Diagram of the phosphotransacetylase (Pta)-acetate kinase (AckA) pathway. acCoA, acetyl-CoA; acP, acetyl phosphate. (B) P_{virB}-*lacZ* expression in *E. coli* strains carrying pRG145/pFQ95 (VirGN54D) or pRG146/pRG149 (VirGI77V/D52E).

Dependence of the activity of VirGN54D on acetyl phosphate in *E. coli*. Since VirGN54D accumulates phosphate independently of VirA and AS, we reasoned that phosphorylation could be mediated either via another histidine kinase through cross talk or metabolically through small-molecule phosphate donors like acetyl phosphate, carbamoyl phosphate, and phosphoramidate, as seen in other response regulators (26, 43). To examine whether acetyl phosphate has any effect on the constitutive activity of VirGN54D, *E. coli* strains were used to exploit the well-characterized acetyl phosphate synthesis pathway. VirGN54D had already been shown to be active in *E. coli* once the α subunit of the RNA polymerase from *A. tumefaciens* was supplied (23).

As shown in Fig. 4A, acetyl phosphate is the intermediate of the phosphotransacetylase-acetate kinase (Pta-AckA) pathway. If AckA is absent, cells produce acetyl phosphate from abundant acetyl-coenzyme A (CoA) but are not able to degrade acetyl phosphate to acetate efficiently, resulting in a higher acetyl phosphate level than in wild-type cells (34, 54). VirGN54D has a higher activity in the strain lacking AckA (AJW1939) than in the wild type (AJW678), while VirGI77V/D52E displays a consistent activity independent of the *ackA* mutation (Fig. 4B). These data implicate the activity of VirGN54D in the dependence of *E. coli* on the acetyl phosphate concentration in the cell.

Gel retardation assays of VirG proteins. DNA fragments containing the *virB* promoter were used to probe the DNA binding ability of purified VirG proteins. Wild-type VirG appeared unable to form a complex with the DNA probe to shift the band under these concentrations (Fig. 5A). Significant amounts of the VirGN54D-DNA complex were only apparent at high protein concentrations (6 μM), while VirGI77V/D52E shifted the DNA band at much lower concentrations (0.6 μM). These data are consistent with a higher DNA binding affinity for VirGI77V/D52E than for VirGN54D. Moreover, a protein-DNA complex with a higher molecular weight was observed with VirGI77V/D52E but not with VirGN54D. The higher-molecular-weight complex may arise from the binding of multiple proteins to two binding sites (*vir* boxes) in the promoter (12). Both *vir* boxes have been shown to be required for activation of the *vir* promoter (51), and the increased DNA binding affinity of VirGI77V/D52E may contribute to the constitutive activity of VirGI77V/D52E.

Structural modeling of VirG. To better understand the constitutive activities of these different alleles, both "unphosphorylated" and "phosphorylated" VirG model structures were generated through homology modeling (Fig. 6). An α/β fold with a five-stranded β sheet and five α helices is well defined in both structural models. N54 is located at the β3-α3 loop, two residues C terminal to the conserved D52, and within the phosphorylation active site. The close proximity to the phosphorylation center and the surface characteristic of the N54

Downloaded from http://jb.asm.org/ on July 19, 2018 by guest

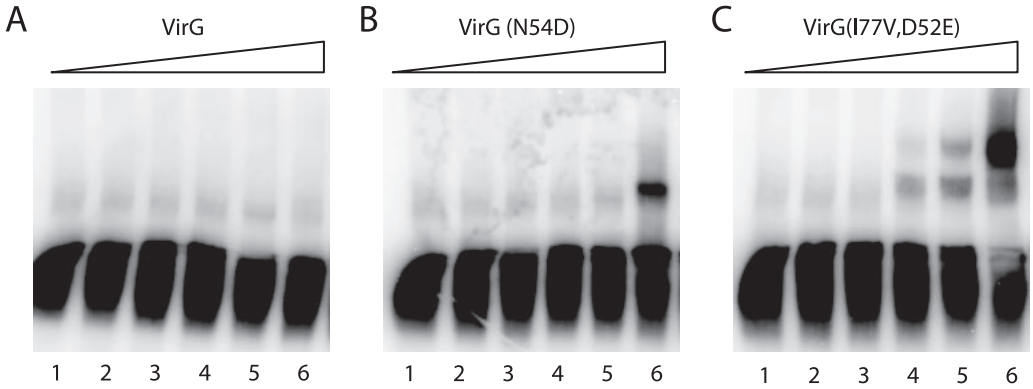

FIG. 5. Gel retardation assay of the binding of *virB* promoter with (A) VirG, (B) VirGN54D, and (C) VirGI77V/D52E. VirG proteins were added to a final concentration of 0 μM (lane 1), 0.1 μM (lane 2), 0.2 μM (lane 3), 0.6 μM (lane 4), 2 μM (lane 5), and 6 μM (lane 6).

residue may well determine the stability of the acyl phosphate and the accessibility of phosphate donors to the site.

An "aromatic switch" involving D52, S79, and F99 is evident in the VirG model structures, as described for other RRs (3, 15, 43). Upon phosphorylation, the conserved S79 reorients its side chain hydroxyl from a position pointing away from the phosphorylation site D52 (Fig. 6A) to a position proximal to the phosphate (Fig. 6B). The formation of a new hydrogen bond with a phosphoryl oxygen atom accompanies the flipping of the side chain of a conserved aromatic residue F99 from an "outward" orientation (Fig. 6A) to an "inward" and buried position (Fig. 6B) that fills the empty space left behind by S79. The movement of the bulky F99 ultimately results in the rearrangement of β4-α4-β5-α5, and these elements are probably involved in regulating the activity of the C-terminal DNA binding domain. The I77 side chain resides just beside S79, on the same face of the β4 strand. A similar reorientation of this side chain is observed in the "phosphorylated" structure model.

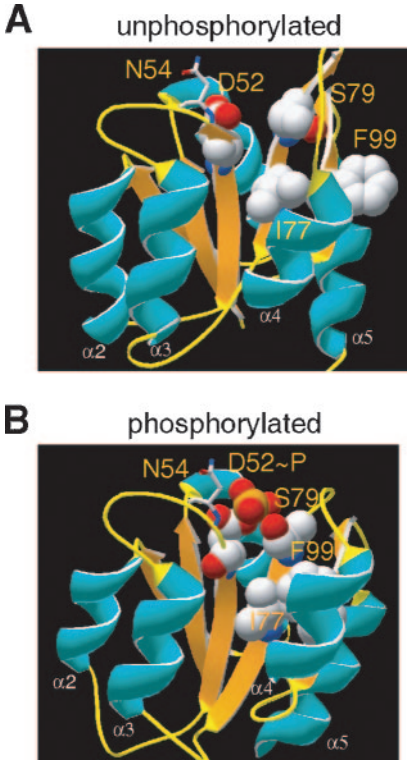

FIG. 6. Model structures of VirG. The structures of VirG before and after the phosphorylation were modeled by SWISS-PROT as described in Material and Methods. Residues involved in the conserved Asp-Ser/Thr-Tyr/Phe (D52-S79-F99) "aromatic switch" (3, 15, 22) were highlighted together with N54 and I77: white, C; red, O; blue, N; orange, P. The N54 residue is shown as sticks for a clear view of the phosphorylation site.

The above analysis is consistent with the I77V mutation decreasing the size of the side chain and creating a space for the side chain of F99 to occupy. Additionally, the D52E mutation extends the carboxyl group and positions the carboxylate oxygen within hydrogen bond distance of the hydroxyl group of S79. Therefore, both structural perturbations caused by I77V and D52E may represent some features of the "active" conformation, and the combination of the two may be required for the constitutive activity of VirGI77V/D52E. Indeed, VirGI77V shows little constitutive activity and remains AS inducible (Fig. 7). This hypothesis was further explored by introducing site-specific mutations at positions 77 and 52. In I77L, this conservative size substitution did not produce a constitutive allele in VirGI77L/D52E. However, in VirGI77A/D52E, which again carries a hydrophobic side chain at position 77 that is smaller than in wild-type VirG, constitutive *vir* expression at a similar

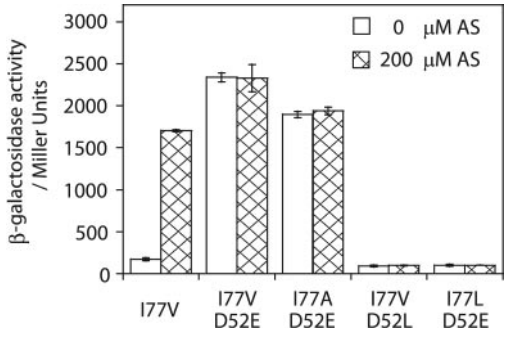

FIG. 7. P_{virB}-*lacZ* expression of VirG mutants. β-Galactosidase activity was assayed for A136(pRG129) strains carrying the following plasmids: (from left to right) pRG111, pRG112b, pB9, pB7, and pB8.

Downloaded from http://jb.asm.org/ on July 19, 2018 by guest

level as VirGI77V/D52E was observed. This model further predicts that replacing the E52 carboxylate with leucine should abolish its ability to form a hydrogen bond with S79, and the resulting VirGI77V/D52L indeed was inactive (Fig. 7).

DISCUSSION

Even in the face of the great diversity of environmental signals being perceived by prokaryotes and the divergent time frames during which these signals must remain active, the highly conserved phosphate-receiving domains of the two-component response regulators suggest a common propagation event regulating signal output. To better understand these structural changes, we have investigated the constitutive mutants of the VirG response regulator. These studies establish that VirGI77V/D52E and VirGN54D have different phosphorylation patterns, distinct DNA binding abilities, and altered regulation of signal output. Nevertheless, these alleles can be understood through a common series of conformational changes regulated by ancillary residues that appear specific to the function of the response regulator. Each constitutive allele is discussed separately below.

VirGI77V/D52E. VirGI77V/D52E was originally discovered as a mutant that restores the activity of VirGD52E (10). In contrast to the low previously reported constitutive activity of *virGI77V/D52E* (10), driving expression behind the strong P_{N25} promoter results in superior constitutive activity. Under these conditions, we show that the conserved residues at the RR phosphorylation center (D52 and D9) are not required for VirGI77V/D52E activity. Rather, the constitutive activity of VirGI77V/D52E seems to originate not from its phosphorylation status but from a structural change mimicking the active conformation. Structural changes that would shift the conformation equilibrium to the active state should directly increase the binding affinity to *vir* promoters, and indeed the gel retardation assays showed VirGI77V/D52E to have higher DNA binding affinity with the *virB* promoter than either VirGN54D or wild-type VirG.

The proposed structural changes induced by the I77V and D52E substitutions are based on our structural modeling of VirG. A decrease in size of the side chain at position 77 and a lengthening of the position of the carboxyl group (E52) to within hydrogen bonding distance with S79 are consistent with the "aromatic switch" conformational change induced by phosphorylation. The constitutive activity of VirGI77A/D52E and the loss of activity in VirGI77L/D52E and VirGI77V/D52L provide further support for the importance of steric positioning of these side chains. Either effect alone appears to be capable of changing the conformation equilibrium. VirGI77V is hypersensitive to AS (36), possibly reflecting such an equilibrium shift, and the D-for-E substitutions at the phosphorylation sites in other RRs are known to generate constitutive alleles (16, 18, 40). Moreover, a M85V substitution in CheY, corresponding to the I77 position in VirG, results in constitutive activation when combined with multiple mutations at other residues (7). However, a single structural change is not sufficient to shift the equilibrium to the level necessary for constitutive activation of VirG, since VirGI77V, VirGD52E, VirGI77L/D52E, and VirGI77V/D52L are not constitutive.

VirGN54D. The constitutive activity of VirGN54D was previously assigned as an additional negative charge in the mutant simulating the phosphorylated state (12, 13). However, we show here that VirGN54D is phosphorylated in vivo, and the phosphorylation is independent of its cognate histidine kinase VirA. Both the phosphorylation and the activity of VirGN54D depend on the D52 and D9 residues at the phosphorylation center, which further underlines the importance of phosphorylation to the activity of VirGN54D. Due to the general instability of acyl phosphates, the purified VirGN54D protein is not likely to carry significant amounts of phosphate through purification. Indeed, the purified protein displays much weaker DNA binding than VirGI77V/D52E even though both mutants are equally active in *vir* expression in vivo. Moreover, even though VirGN54D shows stronger DNA binding affinity than wild-type VirG, it did not form the higher-molecular-weight protein-DNA complexes seen with VirGI77V/D52E, in contrast with the gel retardation assays of MBP-VirGN54D described previously (12). This discrepancy may be due to the maltose binding protein fusion at the N terminal of VirG altering its structure, consistent with the MBP-VirGN54D chimera not being able to activate *vir* expression in *A. tumefaciens*. Taken together, phosphorylation appears to be required for the activity of VirGN54D and the constitutive in vivo activity resulting from phosphorylation by phosphate donors other than VirA.

Small-molecule phosphate donors, such as acetyl phosphate, carbamoyl phosphate, and phosphoramidate, have been shown to phosphorylate response regulators (26, 43), and a similar phosphorylation by acetyl phosphate was reported for the constitutive activity of another RR, PhoPS93N (5). The constitutive activities of VirGN54D are well correlated with the acetyl phosphate levels in *E. coli* strains carrying mutations in *ackA*. Therefore, acetyl phosphate appears to be the source for constitutive phosphorylation of VirGN54D in *E. coli*, although we cannot exclude the possibility that acetyl phosphate indirectly modulates VirGN54D phosphorylation through other two-component pathways. In addition, the *pta* and *ackA* homologs have not been identified in *Agrobacterium*, and the phosphate source for VirGN54D in *A. tumefaciens* may come from acetyl phosphate synthesized via alternative pathways (53) or other small-molecule phosphate donors like carbamoyl phosphate, whose biosynthesis genes are in the genome sequence.

Our structure models place the N54 residue at the β3-α3 loop on the protein surface and close to the D52 site of phosphorylation. As these β-α loops appear to function as the recognition interface between the histidine kinase and its cognate response regulator (46), the N54D mutation might disrupt the VirA-VirG interaction to abolish phosphorylation by VirA (13). On the other hand, this nonconserved position, located two residues C terminal to the conserved aspartate (D + 2 position), appears to play a vital role in the stability of the RR acyl phosphates. Increased phosphorylations for CheYN59R and CheBE58K have been documented, while Spo0FK56N shows a decreased level of phosphorylation (37, 42, 55). The K56N substitution in Spo0F is claimed to accelerate the autophosphatase activity of the RR by facilitating the positioning of a water molecule for the phosphate hydrolysis, and CheBE58K is apparently constitutively active due to decreased autophosphatase activity (55). Finally, the N59R substitution in CheY is

Downloaded from http://jb.asm.org/ on July 19, 2018 by guest

found to form a salt bridge with E89, a residue important in CheZ-mediated dephosphorylation of CheY. Despite the absence of a clear and universal mechanism for altered phosphorylation, the emerging pattern is that D + 2 contributes to the stability of acyl phosphate, and the constitutive activity of VirGN54D may result from enhanced phosphate stability. The VirGN54D phosphate indeed displayed more resistance to acid/base treatment, showing significant phosphate remaining after the acid or base washes that remove phosphates from wild-type VirG (30). The autophosphatase activity of wild-type VirG, which prevents phosphorylation by small-molecule phosphate donors, may well be overwhelmed by N54D.

Finally, a survey of response regulators reveals other examples, including AmfR (45), FimZ (29), CutR (6), and EvgA (31), which contain an Asp residue in the wild-type sequence two residues after the putative phosphorylation site. Curiously, AmfR and FimZ are orphan response regulators without a cognate histidine kinase, and overexpression of EvgA itself can regulate the downstream genes in a strain deficient of the cognate histidine kinase EvgS (29, 31, 45). Taken together, D + 2 appears to be generally critical for cognate histidine kinase specificity, phosphoprotein stability, and phosphatase accessibility.

Constitutive activation of RR. In summary, response regulators can be constitutively activated by extending the lifetime of the phosphorylated state or mimicking the active conformation. VirGN54D and VirGI77V/D52E represent the two extremes: VirGN54D relies on constitutive phosphorylation, and VirGI77V/D52E mimics the structural changes of the phosphorylation-induced conformation. Interestingly, both I77 and N54 are at positions not highly conserved among RRs. Position 54 is at the β3-α3 loop in close proximity of the phosphorylated aspartate, and the backbone amide in fact participates in a hydrogen bond with a phosphate oxygen. The residues at this position are diverse among RRs, possibly reflecting different conformational equilibria for different RRs, yet various reports have repeatedly indicated a common role for this residue in altering the stability of the acyl phosphate. Similarly, position 77 is at the β4 strand and is usually occupied by various hydrophobic residues (M, L, V, I, and F). The structure proximity of this position to the highly conserved residues of the "aromatic switch" implicates this residue in adjusting the effectiveness of conformation propagation. It seems that both positions 54 and 77 have roles of regulating the lifetime of the active conformation within the active/inactive equilibrium.

This conserved conformation/propagation pathway among response regulators may well determine a common set of positions that perturb the active/inactive equilibrium. A diverse set of residues proximal to these positions now appear to contribute to different lifetimes of the individual RRs, and these are adapted to their individual biological roles. Analysis and comparison of constitutive RR mutants reveal the identity of such positions and extend our understanding of signal regulation. That said, while a universal set of rules have not yet emerged (40), these patterns do suggest that it will be possible to combine multiple elements to engineer altered signaling lifetimes and novel responses within a wide array of functional outputs.

ACKNOWLEDGMENTS

We thank Alan J. Wolfe, Loyola University Chicago, and Anath Das, University of Minnesota, for providing strains, Andrew Binns and his laboratory at University of Pennsylvania for insight and advice, and NIH (GM47369) for support.

REFERENCES

1. **Benda, C., C. Scheufler, N. T. de Marsac, and W. Gartner.** 2004. Crystal structures of two cyanobacterial response regulators in apo- and phosphorylated form reveal a novel dimerization motif of phytochrome-associated response regulators. Biophys. J. **87:**476–487.
2. **Birck, C., Y. Chen, F. M. Hulett, and J.-P. Samama.** 2003. The crystal structure of the phosphorylation domain in PhoP reveals a functional tandem association mediated by an asymmetric interface. J. Bacteriol. **185:**254–261.
3. **Birck, C., L. Mourey, P. Gouet, B. Fabry, J. Schumacher, P. Rousseau, D. Kahn, and J. P. Samama.** 1999. Conformational changes induced by phosphorylation of the FixJ receiver domain. Structure **7:**1505–1515.
4. **Cangelosi, G. A., E. A. Best, G. Martinetti, and E. W. Nester.** 1991. Genetic analysis of Agrobacterium. Methods Enzymol. **204:**384–397.
5. **Chamnongpol, S., and E. A. Groisman.** 2000. Acetyl phosphate-dependent activation of a mutant PhoP response regulator that functions independently of its cognate sensor kinase. J. Mol. Biol. **300:**291–305.
6. **Chang, H. M., M. Y. Chen, Y. T. Shieh, M. J. Bibb, and C. W. Chen.** 1996. The cutRS signal transduction system of Streptomyces lividans represses the biosynthesis of the polyketide antibiotic actinorhodin. Mol. Microbiol. **21:**1075–1085.
7. **Da Re, S., T. Tolstykh, P. M. Wolanin, and J. B. Stock.** 2002. Genetic analysis of response regulator activation in bacterial chemotaxis suggests an intermolecular mechanism. Protein Sci. **11:**2644–2654.
8. **Gao, R., and D. G. Lynn.** 2005. Environmental pH sensing: resolving the VirA/VirG two-component system inputs for *Agrobacterium* pathogenesis. J. Bacteriol. **187:**2182–2189.
9. **Gardino, A. K., B. F. Volkman, H. S. Cho, S. Y. Lee, D. E. Wemmer, and D. Kern.** 2003. The NMR solution structure of BeF(3)(-)-activated Spo0F reveals the conformational switch in a phosphorelay system. J. Mol. Biol. **331:**245–254.
10. **Gubba, S., Y. H. Xie, and A. Das.** 1995. Regulation of *Agrobacterium tumefaciens* virulence gene expression: isolation of a mutation that restores virGD52E function. Mol. Plant-Microbe Interact. **8:**788–791.
11. **Han, D. C., C. Y. Chen, Y. F. Chen, and S. C. Winans.** 1992. Altered-function mutations of the transcriptional regulatory gene *virG* of *Agrobacterium tumefaciens*. J. Bacteriol. **174:**7040–7043.
12. **Han, D. C., and S. C. Winans.** 1994. A mutation in the receiver domain of the *Agrobacterium tumefaciens* transcriptional regulator VirG increases its affinity for operator DNA. Mol. Microbiol. **12:**23–30.
13. **Jin, S., Y. Song, S. Q. Pan, and E. W. Nester.** 1993. Characterization of a *virG* mutation that confers constitutive virulence gene expression in Agrobacterium. Mol. Microbiol. **7:**555–562.
14. **Jin, S. G., R. K. Prusti, T. Roitsch, R. G. Ankenbauer, and E. W. Nester.** 1990. Phosphorylation of the VirG protein of *Agrobacterium tumefaciens* by the autophosphorylated VirA protein: essential role in biological activity of VirG. J. Bacteriol. **172:**4945–4950.
15. **Johnson, L. N., and R. J. Lewis.** 2001 Structural basis for control by phosphorylation. Chem. Rev. **101:**2209–2242.
16. **Klose, K. E., D. S. Weiss, and S. Kustu.** 1993. Glutamate at the site of phosphorylation of nitrogen-regulatory protein NTRC mimics aspartyl-phosphate and activates the protein. J. Mol. Biol. **232:**67–78.
17. **Kumari, S., C. M. Beatty, D. F. Browning, S. J. W. Busby, E. J. Simel, G. Hovel-Miner, and A. J. Wolfe.** 2000. Regulation of acetyl coenzyme A synthetase in *Escherichia coli*. J. Bacteriol. **182:**4173–4179.
18. **Lan, C.-Y., and M. M. Igo.** 1998. Differential expression of the OmpF and OmpC porin proteins in *Escherichia coli* K-12 depends upon the level of active OmpR. J. Bacteriol. **180:**171–174.
19. **Lee, K., M. W. Dudley, K. M. Hess, D. G. Lynn, R. D. Joerger, and A. N. Binns.** 1992. Mechanism of activation of Agrobacterium virulence genes: identification of phenol-binding proteins. Proc. Natl. Acad. Sci. USA **89:**8666–8670.
20. **Lee, S.-Y., H. S. Cho, J. G. Pelton, D. Yan, E. A. Berry, and D. E. Wemmer.** 2001. Crystal structure of activated CheY. Comparison with other activated receiver domains. J. Biol. Chem. **276:**16425–16431.
21. **Lee, S. Y., H. S. Cho, J. G. Pelton, D. Yan, R. K. Henderson, D. S. King, L. Huang, S. Kustu, E. A. Berry, and D. E. Wemmer.** 2001. Crystal structure of an activated response regulator bound to its target. Nat. Struct. Biol. **8:**52–56.
22. **Lewis, R. J., J. A. Brannigan, K. Muchova, I. Barak, and A. J. Wilkinson.** 1999. Phosphorylated aspartate in the structure of a response regulator protein. J. Mol. Biol. **294:**9–15.
23. **Lohrke, S. M., S. Nechaev, H. Yang, K. Severinov, and S. J. Jin.** 1999. Transcriptional activation of *Agrobacterium tumefaciens* virulence gene promoters in *Escherichia coli* requires the *A. tumefaciens* RpoA gene, encoding the alpha subunit of RNA polymerase. J. Bacteriol. **181:**4533–4539.

Downloaded from http://jb.asm.org/ on July 19, 2018 by guest

24. **Lohrke, S. M., H. Yang, and S. Jin.** 2001. Reconstitution of acetosyringone-mediated *Agrobacterium tumefaciens* virulence gene expression in the heterologous host *Escherichia coli*. J. Bacteriol. **183:**3704–3711.
25. **Lukat, G. S., B. H. Lee, J. M. Mottonen, A. M. Stock, and J. B. Stock.** 1991. Roles of the highly conserved aspartate and lysine residues in the response regulator of bacterial chemotaxis. J. Biol. Chem. **266:**8348–8354.
26. **Lukat, G. S., W. R. McCleary, A. M. Stock, and J. B. Stock.** 1992. Phosphorylation of bacterial response regulator proteins by low molecular weight phospho-donors. Proc. Natl. Acad. Sci. USA **89:**718–722.
27. **Meyer, M. G., S. Park, L. Zeringue, M. Staley, M. McKinstry, R. I. Kaufman, H. Zhang, D. Yan, N. Yennawar, H. Yennawar, G. K. Farber, and B. T. Nixon.** 2001. A dimeric two-component receiver domain inhibits the sigma54-dependent ATPase in DctD. FASEB J. **15:**1326–1328.
28. **Miller, J. H.** 1972. Experiments in molecular genetics. Cold Spring Harbor Laboratory Press, Cold Spring Harbor, N.Y.
29. **Mizuno, T.** 1997. Compilation of all genes encoding two-component phosphotransfer signal transducers in the genome of *Escherichia coli*. DNA Res. **4:**161–168.
30. **Mukhopadhyay, A., R. Gao, and D. G. Lynn.** 2004. Integrating input from multiple signals: the VirA/VirG two component system of *Agrobacterium tumefaciens*. Chembiochem **5:**1535–1542.
31. **Nishino, K., and A. Yamaguchi.** 2001. Overexpression of the response regulator *evgA* of the two-component signal transduction system modulates multidrug resistance conferred by multidrug resistance transporters. J. Bacteriol. **183:**1455–1458.
32. **Park, S., M. Meyer, A. D. Jones, H. P. Yennawar, N. H. Yennawar, and B. T. Nixon.** 2002. Two-component signaling in the AAA + ATPase DctD: binding Mg2+ and BeF3− selects between alternate dimeric states of the receiver domain. FASEB J. **16:**1964–1966.
33. **Pazour, G. J., C. N. Ta, and A. Das.** 1992. Constitutive mutations of *Agrobacterium tumefaciens* transcriptional activator *virG*. J. Bacteriol. **174:**4169–4174.
34. **Pruss, B. M., and A. J. Wolfe.** 1994. Regulation of acetyl phosphate synthesis and degradation, and the control of flagellar expression in Escherichia coli. Mol. Microbiol. **12:**973–984.
35. **Rodenburg, K. W., E. Scheeren-Groot, G. Vriend, and P. J. Hooykaas.** 1994. The N-terminal domain of VirG of *Agrobacterium tumefaciens*: modelling and analysis of mutant phenotypes. Protein Eng. **7:**905–909.
36. **Scheeren-Groot, E. P., K. W. Rodenburg, A. den Dulk-Ras, S. C. Turk, and P. J. Hooykaas.** 1994. Mutational analysis of the transcriptional activator VirG of *Agrobacterium tumefaciens*. J. Bacteriol. **176:**6418–6426.
37. **Silversmith, R. E., J. G. Smith, G. P. Guanga, J. T. Les, and R. B. Bourret.** 2001. Alteration of a nonconserved active site residue in the chemotaxis response regulator CheY affects phosphorylation and interaction with CheZ. J. Biol. Chem. **276:**18478–18484.
38. **Simonovic, M., and K. Volz.** 2001. A distinct meta-active conformation in the 1.1-A resolution structure of wild-type ApoCheY. J. Biol. Chem. **276:**28637–28640.
39. **Smith, J. G., J. A. Latiolais, G. P. Guanga, S. Citineni, R. E. Silversmith, and R. B. Bourret.** 2003. Investigation of the role of electrostatic charge in activation of the *Escherichia coli* response regulator CheY. J. Bacteriol. **185:**6385–6391.
40. **Smith, J. G., J. A. Latiolais, G. P. Guanga, J. D. Pennington, R. E. Silversmith, and R. B. Bourret.** 2004. A search for amino acid substitutions that universally activate response regulators. Mol. Microbiol. **51:**887–901.
41. **Sola, M., F. X. Gomis-Ruth, L. Serrano, A. Gonzalez, and M. Coll.** 1999. Three-dimensional crystal structure of the transcription factor PhoB receiver domain. J. Mol. Biol. **285:**675–687.
42. **Stewart, R.** 1993. Activating and inhibitory mutations in the regulatory domain of CheB, the methylesterase in bacterial chemotaxis. J. Biol. Chem. **268:**1921–1930.
43. **Stock, A. M., and A. H. West.** 2003. Response regulator proteins and their interactions with histidine protein kinases, p. 237–271. *In* M. Inouye and R. Dutta (ed.), Histidine kinases in signal transduction. Academic Press, San Diego, Calif.
44. **Tzfira, T., and V. Citovsky.** 2002. Partners-in-infection: host proteins involved in the transformation of plant cells by Agrobacterium. Trends Cell Biol. **12:**121–129.
45. **Ueda, K., K. Miyake, S. Horinouchi, and T. Beppu.** 1993. A gene cluster involved in aerial mycelium formation in *Streptomyces griseus* encodes proteins similar to the response regulators of two-component regulatory systems and membrane translocators. J. Bacteriol. **175:**2006–2016.
46. **Varughese, K. I.** 2002. Molecular recognition of bacterial phosphorelay proteins. Curr. Opin. Microbiol. **5:**142–148.
47. **Volkman, B. F., D. Lipson, D. E. Wemmer, and D. Kern.** 2001. Two-state allosteric behavior in a single-domain signaling protein. Science **291:**2429–2433.
48. **Wang, Y., A. Mukhopadhyay, V. R. Howitz, A. N. Binns, and D. G. Lynn.** 2000. Construction of an efficient expression system for *Agrobacterium tumefaciens* based on the coliphage T5 promoter. Gene **242:**105–114.
49. **Watson, B., T. C. Currier, M. P. Gordon, M. D. Chilton, and E. W. Nester.** 1975. Plasmid required for virulence of *Agrobacterium tumefaciens*. J. Bacteriol. **123:**255–264.
50. **West, A. H., and A. M. Stock.** 2001. Histidine kinases and response regulator proteins in two-component signaling systems. Trends Biochem. Sci. **26:**369–376.
51. **Winans, S. C.** 1990. Transcriptional induction of an *Agrobacterium* regulatory gene at tandem promoters by plant-released phenolic compounds, phosphate starvation, and acidic growth media. J. Bacteriol. **172:**2433–2438.
52. **Winans, S. C., N. J. Mantis, C. Y. Chen, C. H. Chang, and D. C. Han.** 1994. Host recognition by the VirA, VirG two-component regulatory proteins of *Agrobacterium tumefaciens*. Res. Microbiol. **145:**461–473.
53. **Wolfe, A. J.** 2005. The acetate switch. Microbiol. Mol. Biol. Rev. **69:**12–50.
54. **Wolfe, A. J., D.-E. Chang, J. D. Walker, J. E. Seitz-Partridge, M. D. Vidaurri, C. F. Lange, B. M. Pruss, M. C. Henk, J. C. Larkin, and T. Conway.** 2003. Evidence that acetyl phosphate functions as a global signal during biofilm development. Mol. Microbiol. **48:**977–988.
55. **Zapf, J., M. Madhusudan, C. E. Grimshaw, J. A. Hoch, K. I. Varughese, and J. M. Whiteley.** 1998. A source of response regulator autophosphatase activity: the critical role of a residue adjacent to the Spo0F autophosphorylation active site. Biochemistry **37:**7725–7732.
56. **Zhu, J., P. M. Oger, B. Schrammeijer, P. J. Hooykaas, S. K. Farrand, and S. C. Winans.** 2000. The bases of crown gall tumorigenesis. J. Bacteriol. **182:**3885–3895.

Downloaded from http://jb.asm.org/ on July 19, 2018 by guest